

## Application of laser Scribed method to fabricate graphene/graphene oxide multilayer

M. Namdar, Sh. Kh. Asl\*

New materials Lab., University of Tabriz, Tabriz, Iran

\*) E-mail: [sshahab\\_kh@yahoo.com](mailto:sshahab_kh@yahoo.com)

Received 11/8/2018, Accepted 22/12/2018, Accepted 15/1/2019



Graphene is a flat layer of carbon atom, and is a layer of graphite with a thickness of a few tenths of a nanometer that due to its porous structure and high ionic transfer rate, it has been considered in electronic applications, such as cloud storage capacitors with high energy. In this research work, laser scribed technique has been regarded to synthesize graphene on the surface of a DVD and manufacture graphene and graphene composite super capacitors with Molybdenum disulfide. For this purpose, first, by Hummer's method, graphite was converted to graphene oxide (GO) in an acidic environment containing Sodium nitrate, Potassium permanganate and sulfuric acid. Centrifuges and ultrasonic devices were utilized for the homogenization of graphene oxide solution. GO homogeneous solution was applied on the surface of specific DVDs and the set was dried at room temperature. For GO reduction and transform it into graphene, a suitable laser, with programming of super capacitor particular pattern was used. By applying energy with the amount of resonance frequency of graphene and oxygen bond, the laser broke the connection and the reduction action and reaching to graphene was done. Thus, the optimal wavelength of laser was determined to reduce the GO. In this study, the process of graphene synthesis and applying the super capacitor specific pattern were carried out in single step that is the biggest advantage of laser scribed graphene (LSG) method. In present study, TEM was utilized to examine the layered structure of GO, SEM was used for microstructural studies the XPS was used to investigate elements present in the layer applied on DVD, and the Raman spectroscopy was applied to investigate the quality of prepared graphene through studying G and D peaks., two tests of cyclic voltammetry (CV) and Galvano static charge/discharge (CC) were applied to study the performance and power of energy storage in super capacitors, Finally the long-term charge-discharge stability of the LSG was plotted which indicates that specific capacitance has decreased very slightly from its primary capacitance of  $\sim 10 \text{ F cm}^{-3}$  and its cyclic stability is favorable over 1000 cycles.

**Keywords:** Graphene; Laser Scribed; Lithography; Synthesis; Hummers method.

### 1. INTRODUCTION

Nowadays an increasing use of portable electronic devices can be seen in industrial and experimental applications, medical equipment's and even daily used cell phones and laptops in which the power storage and power durability is a must-have specification of all these devices [1-2]. Miniaturized power storage devices are applied in these devices, where batteries and supercapacitors are the most used ones. Fast charge and discharge beside long cycle life and high-power density are the three properties to make supercapacitors attract more attention than batteries [3-4]. Carbon based materials play important role in manufacturing supercapacitor electrodes and have been heavily investigated [5]. Graphene, a 2D allotrope of carbon, possesses unique electrical and mechanical properties such as outstanding electrical conductivity, very high theoretical surface area of 2630 m<sup>2</sup>/g, promising flexibility and tensile strength of 130 GPa. Thus, graphene Nano-flakes are believed to be suitably applicable in supercapacitor and other energy storage devices [6-9]. Optical properties of bilayer, chair-like and boat-like graphenes investigated by Reshak's group [10, 11], or magnetic properties of doped grapheme studied in other cases [12, 13]. The drawback of using graphene, however, is its restacking tendency after exposure to electrolyte [14,15].

It has been observed that production of graphene derivatives such as graphene oxide (GO) are more convenient than graphene sheets [16]. GO could be chemically [17] or thermally [18] reduced to form graphene. The reduced graphene oxide will contain numerous defect sites, which are favorable for electrochemical applications [19]. A recently invented method of reducing graphene oxide by Kadyetal shows promising advantages over conventional techniques for energy storage applications. They use commercially available Light-scribe DVD burner drivers to convert graphene oxide (GO) into reduced graphene oxide (rGO). The IR laser diode of the optical driver irradiates laser beam with a wavelength of 780 nm, which forces oxygen atoms to leave the graphene oxide structure. The resultant reduced graphene oxide called LSG (lightscribe graphene) is highly defective so that it possesses excellent performance as a supercapacitor [20].

By controlling the laser beam it is possible to pattern desired features on the graphene oxide [21, 22]. Kady et al used this technique to fabricate inter interdigitate electrodes showing them as plausible candidates for flexible energy storage devices [23]. On the other hand, Tianet al facilitated LSG to build planar transistors, photo detector, load speakers and pressure and strain sensors concluding that wafer scale direct printing of graphene-based devices can be achieved by Light scribe optical drives [24-27]. Electrochemical properties of LSG have been investigated by Griffiths etal. They take the advantage of highly effective surfaces of LSG's to fabricate working electrode with fastest heterogeneous electron transfer rate even in comparison with commercial ready edge plane pyrolytic graphite (EPPG) and basal plane pyrolytic graphite (BPPG), and illustrate that the LSG's fabrication method is inexpensive, scalable and compatible with disposable biosensor format [28].

## **2. METHOD OF ANALYSIS**

The resulting suspension was uniformly drop cast on the laser-scribing DVD disk and then dried under air ambient. The GO coated DVD disk was placed in a LightScribe DVD drive with a wavelength of 780nm and a spot size of 20 $\mu$ m. The reduced composite was separated from DVD disk and was glued to the polyethylene terephthalate (PET) substrate. As prepared electrodes were wired out by copper wire using silver paste and the exposed areas of silver paste to electrolyte were passivated.

The electrochemical properties of GO/rGO supercapacitor working electrodes were evaluated in a three-electrode system with platinum rod as counter electrode, a standard Ag/AgCl electrode as reference electrode and 0.5M KCL solution as electrolyte. Cyclic voltammetry (CV) at

different scan rates and galvanostatic charge-discharge at various current densities were carried out on a potentiostat/galvanostat system. The Electrochemical Impedance Spectroscopy (EIS) measurements were performed in the frequency range from 0.1 Hz to 100 kHz with 5mV ac amplitude at open circuit potential. Furthermore, the laser scribing process was utilized to pattern GO/rGO composite onto interdigitated electrodes for the fabrication of flexible micro supercapacitors. Copper tapes were glued to the patterned electrodes. The gel electrolyte for the microsupercapacitor was composed of KCl and PAAK polymer. 2g PAAK was added to 2mL 0.5M KCl solution under vigorous stirring, until a clear solution was obtained. A proper amount of gel electrolyte was dropped on the sample and then spin coated at 2000 rpm for 30sec to create a uniform gel electrolyte surface. CV curves and galvanostatic charge and discharge profiles of GO/rGO based micro supercapacitor were taken between cut-off voltages of 0 and 1 V using the two electrode systems. Figure 1 illustrates the schematic representation of the fabrication process for the flexible micro-supercapacitor.

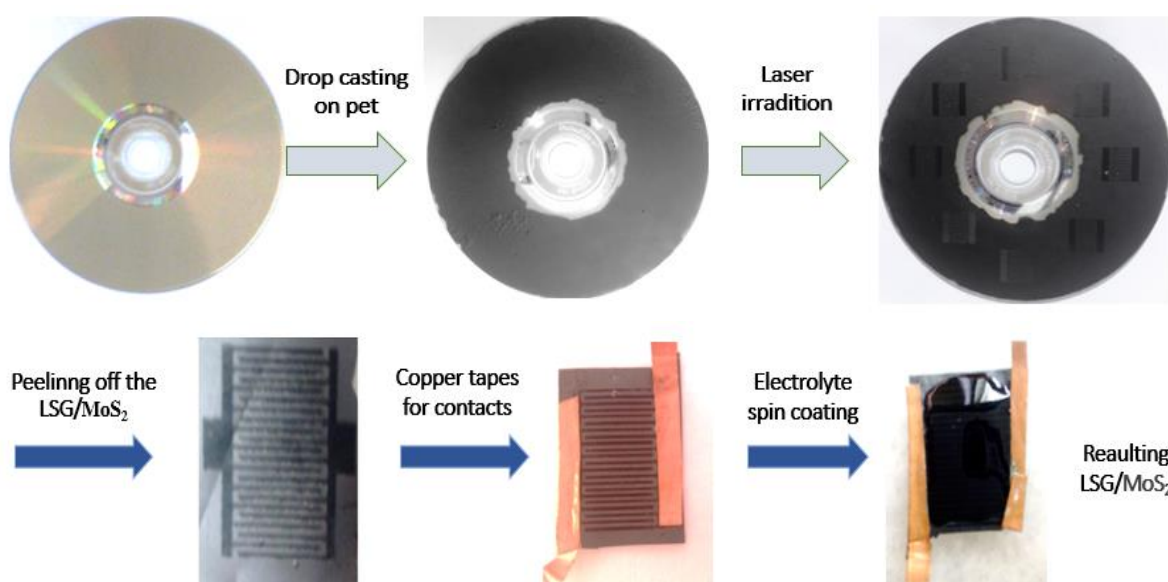


**Figure 1** Schematic representation of flexible micro-supercapacitor (LSG) fabrication.

### 3. EXPERIMENTAL PROCEDURE

GO was prepared by the modified Hummers' method as reported elsewhere [10]. Briefly, 2g graphite powders were added to a mixture of 1g  $\text{NaNO}_3$  and 46ml  $\text{H}_2\text{SO}_4$  and the mixture was cooled to 10 °C using an ice bath. In the next step, 6g  $\text{KMnO}_4$  was gradually added to the above solution and the reaction temperature was maintained below 20 °C. The mixture was then stirred at 35 °C for 2 h. The resulting solution was diluted by adding 92 ml of water until a dark brown suspension was obtained. Then, the solution was treated by adding 340ml  $\text{H}_2\text{O}_2$  solution. The resulting graphite oxide suspension was washed several times by 10% HCl aqueous solution and then by distilled water. Finally, a uniform suspension of GO nanosheets was obtained by adding water to the resulting precipitate and 12h sonicating. The obtained slurry was centrifuged at 1,500 rpm for 45 min, and the top 1/2 supernatant was collected. The collected supernatant was further centrifuged at 3,000 rpm for another 45 min.

To produce a GO/DMF solution, GO was directly added to DMF at an initial concentration of 0.2 mg  $\text{mL}^{-1}$ , and then subjected to gentle sonication at 100 W for 60 min. The obtained GO/DMF solution was brilliant yellow, and could stand for weeks without obvious precipitates

#### 4. RESULTS AND DISCUSSION

In the Raman spectra of the GO and the LSG are shown in Figures 2a and 2b. As can be seen in the figure, both the graphene oxide and the laser scribed graphene exhibit typical disorder D bands at around  $1350\text{ cm}^{-1}$ . Although, graphitic G bands and amorphous 2D bands existing at  $1585\text{ cm}^{-1}$  and  $2360\text{ cm}^{-1}$  can be found in both the GO and the LSG. Our LSG has a lower structural  $\text{sp}^3$  defects as there is a slight decrease in relative intensity of ID/IG after laser scribing. This figure although presents the fact that few layers of graphene were generated after laser irradiation as can be deduced from the increase in relative intensity of 2D band [29].

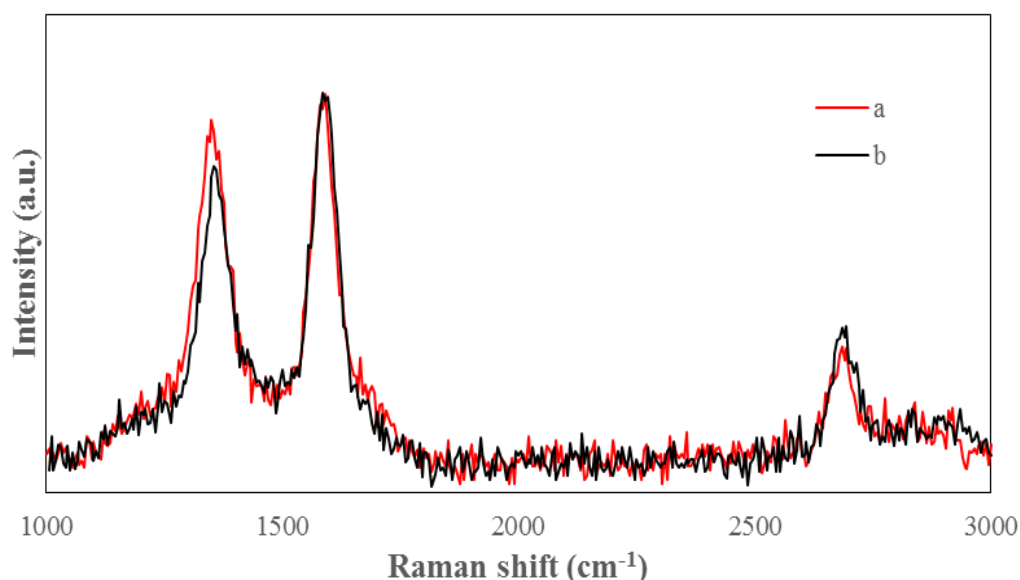


**Figure 2** Raman spectra of graphene nanosheets, before (a) and after (b) laser irradiation.

The comparison of bonding configuration of carbon and oxygen before and after the laser treatment of GO is presented through the following XPS study. Figure 3 shows XPS results of graphene oxide and laser scribed graphene. Laser irradiation causing disappearance of the intense peak around 287eV, which is attributed to  $\text{sp}^3$ -type carbons, indicates that majority of carbonyl and hydroxyl groups were removed by laser irradiation [23, 24]. Another peak removed after laser irradiation was again around 287eV, causing noticeable decrement in ratio of oxygen to carbon which indicates reduction of GO to rGO, followed by turning into rGO sheets.

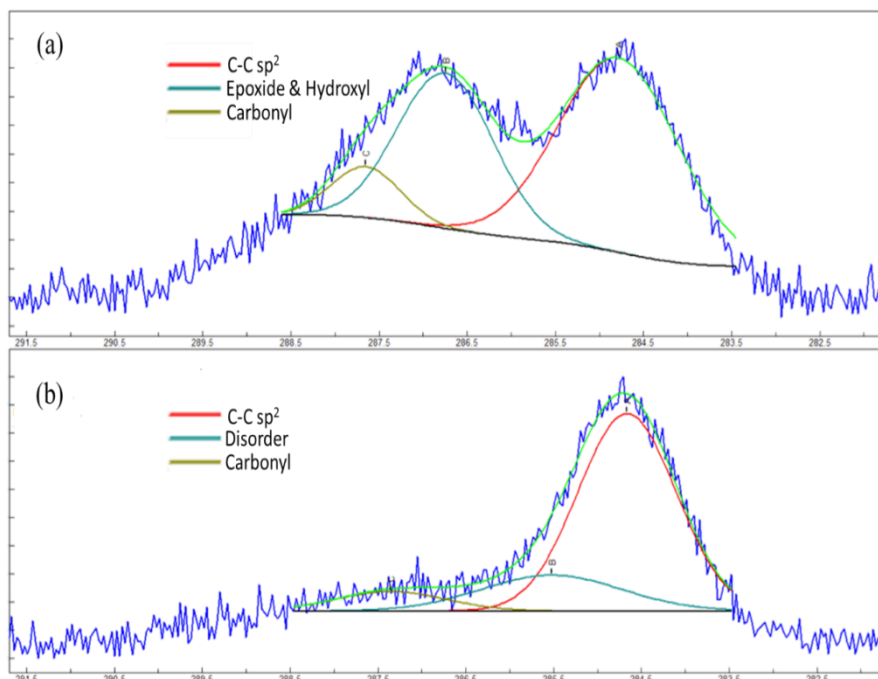


**Figure 3** XPS results of graphene nanosheets, before (a) and after (b) laser irradiation.

Fig. 4 illustrates laser-scribed surface of graphene oxide, indicating how the laser scribe method works. Graphene synthesis and giving the supercapacitor pattern are occurred simultaneously, which is considered to be the principal advantage of this method. Laser beam diameter is approximately 19.9  $\mu\text{m}$  and the distance between adjacent scratches is about 4.6  $\mu\text{m}$ . The reduction of GO is clearly seen in Fig. 4 (c) and Fig. 4 (d). Fig. 4 (c) demonstrates the formation of graphene sheets, and generally the plane state is observable, and the Fig. 4 (d) shows that these formed sheets possess a distance between them and are not stuck together so that ionic exchanges and relocations are carried out.

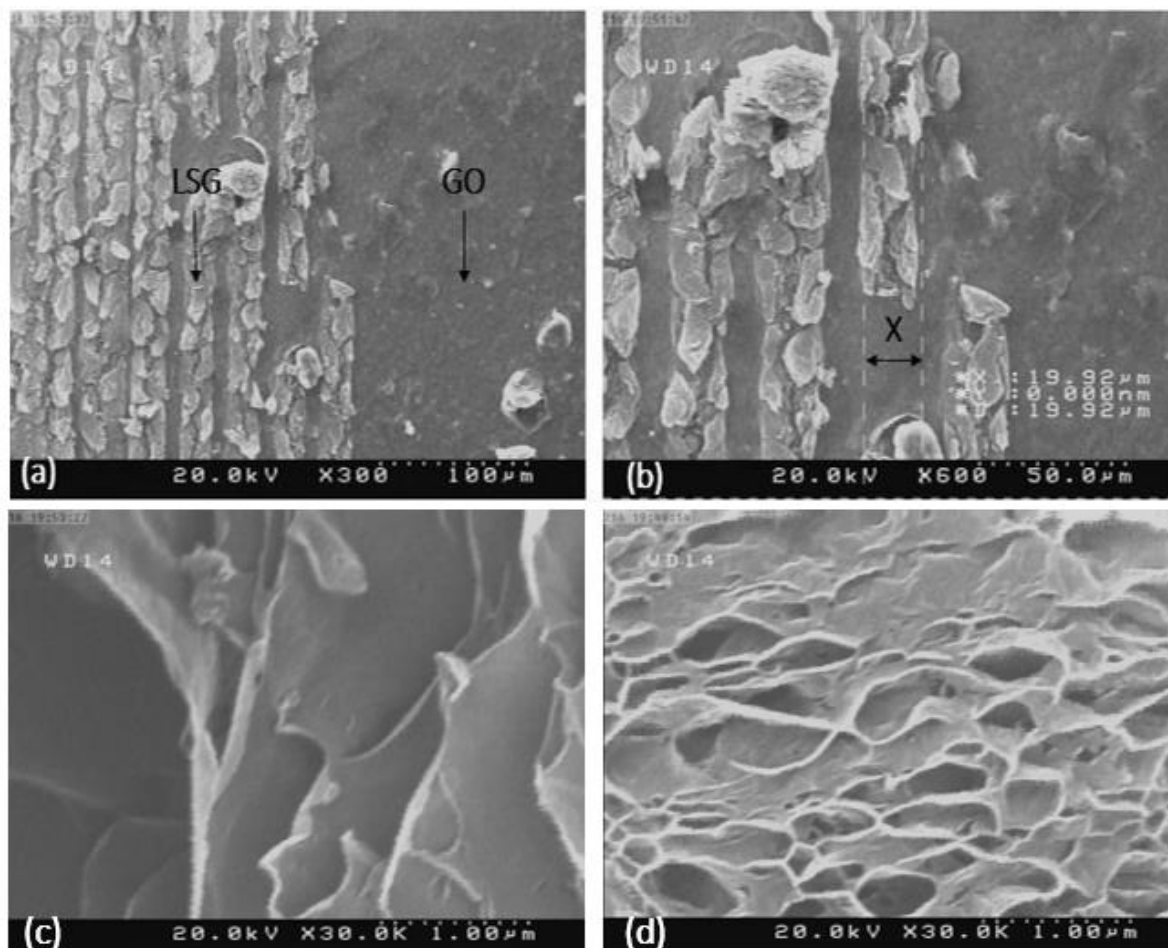


**Figure 4** SEM images of the laser scribed surface of graphene oxide at a low (a) and a high (b) magnification. Reduction of GO and the formation of graphene sheets (c) with a clear distance between them (d).

To investigate the supercapacitance operation of GO/rGO composites with different mass ratios, their electrochemical properties have been investigated. For this aim,, the CV curves of GO/rGO composites were taken between cut-off voltages of 0 and 1 V versus Ag/AgCl reference electrode at different scan rates from 10 (mV/s) to 200 (mV/s). These curves are gathered in Figure 5. it could be understood that fabricated supercapacitor possesses a stored power, and it could be seen at various voltages after testing for 5 times. Since this is a V-I diagram and the internal area of diagram indicates the stored power ( $P=V \cdot I$ ), it could be mentioned assertively that a supercapacitor has been fabricated.

By comparing this CV patterns with a similar work of Maher F. El-Kady et al. [20] which has been illustrated in Fig. 6, based on the inner area of the V-I diagram that is equal with the storing power, it could be concluded that this manufactured supercapacitor possesses a higher storage power.

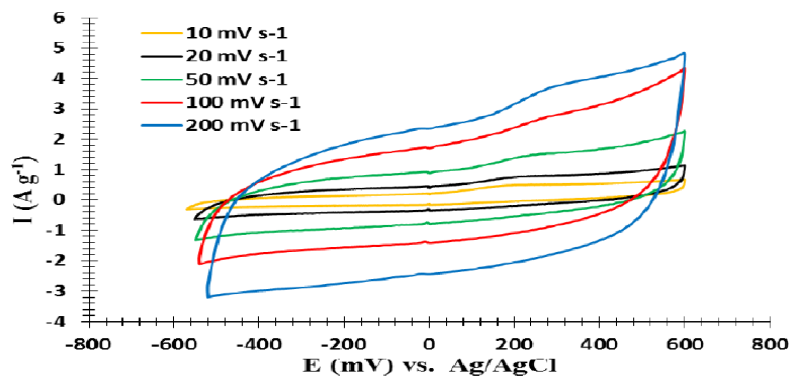


**Figure 5** CV curves of GO/rGO composites at scan rate of 10, 20, 50, 100 and 200 mV/sec in a voltage range of 0 and 1000mV in a three-electrode system.

For further investigations of proposed electrodes, the galvanostatic charge-discharge characteristic of five samples at different current densities are illustrated in Figure 6. As shown in Figure 6, longer time is needed for discharging multilayer.

The specific capacitance of different electrodes can be calculated based on the following equation [30]:

$$C_m = \frac{I \times \Delta t}{\Delta V} \quad (\text{eq.1})$$

where  $I$  refers to the discharge current density ( $\text{A}/\text{cm}^2$ ),  $\Delta t$  is the discharge time, and  $\Delta V$  is the discharge potential range (V). The galvanostatic CC curves have been illustrated in Fig. 6. It is obvious that the specimen has absorbed the energy and returned it to the circuit which has been tested twice. For determining the specific capacitance of this specimen, the following calculations have been made:

For  $I = 1 \text{ A g}^{-1}$ :

$$C_m = \frac{I \times \Delta t}{\Delta V} = \frac{1 \times 6}{600 \times 10^{-3}} = 10 \text{ F g}^{-1}$$

For  $I = 0.1 \text{ A g}^{-1}$ :

$$C_m = \frac{I \times \Delta t}{\Delta V} = \frac{0.1 \times 58}{600 \times 10^{-3}} = 9.7 \sim 10 \text{ F g}^{-1}$$

The specific capacitance of specimen has reached the amount of  $10 \text{ F g}^{-1}$  and has the capability to function as a supercapacitor.

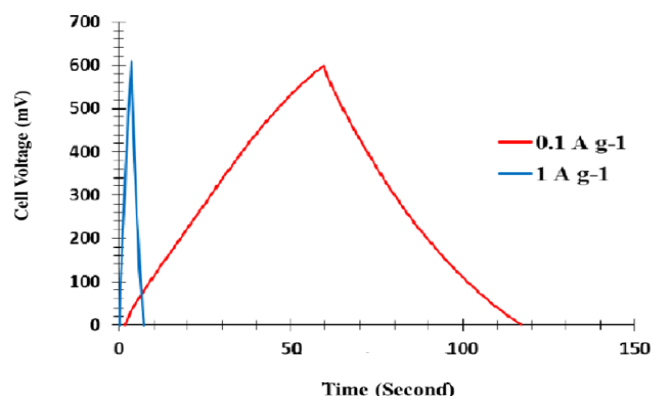


**Figure 6** Charge discharge curves of GO/rGO composites at current density of 0.1, and 1 mA/cm<sup>2</sup> in a voltage range of 0 - 1000mV in a three-electrode system.

The long-term charge discharge stability of the GO/rGO composites were also investigated over 1000 cycles at a current density of  $0.5 \text{ mA/cm}^2$  between cut-off voltages of 0 and 1V versus Ag/AgCl reference electrode and are illustrated in Figure 7. It can be observed that the GO/rGO consequences in larger specific capacitance of the electrode, at the price of deterioration in capacity retention. However, even at the end of 1000<sup>th</sup> cycle, the specific capacitance of GO/rGo composite is about 10 F/g.

The long-term charge-discharge stability and capacitance retention over 5000 cycles was investigated by Wen, Fusheng, et al. [29] for LSG/SWCNTs-MSC By considering our resultant stability diagram, it could be mentioned that capacity decrease in Wen, Fusheng, et al. [29] after 1000 cycles is a bit higher than what we have achieved in Fig. 7. The capacity retention in our study reaches approximately 95 % after 1000 cycles which is quite satisfactory and close to the optimal amount of 98 % after 1000 cycles.

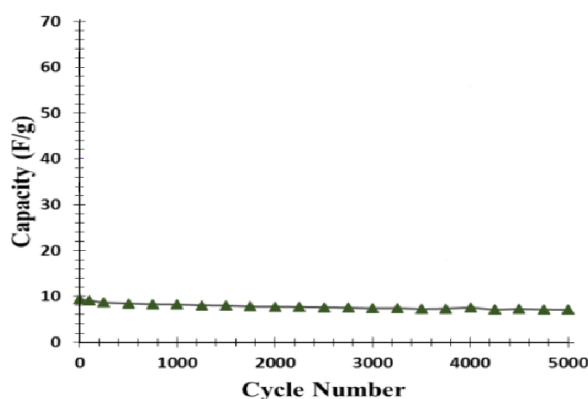


**Figure 7** long-term charge discharge stability of GO/rGO composites at current density of  $0.5 \text{ mA/cm}^2$  in a voltage range of 0 and 1000mV in a three electrode system.

For this case, fabrication of laser-scribed micro supercapacitor electrode was accomplished which is illustrated in Figure 8. This micro supercapacitor is composed of 20 interdigitated electrodes of GO/rGO, separated by insulating spacers of GO/rGO.

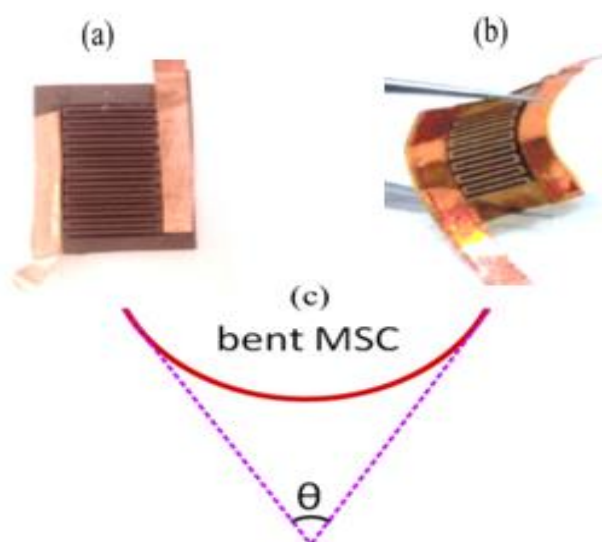


**Figure 8** Optical image of GO/rGO electrode (a). An optical photograph showing the flexibility of the MSC electrode (b) and the bending angle representation for MSC electrode(c).



A comparison of the specific capacitance of LSG supercapacitors has been provided in Table 1. The cross-section image of the LSG exposes a thickness of about 7 ( $\mu\text{m}$ ). The volumetric capacity of LSG multilayers was computed based on the areal capacitance and the cross section image. Our calculations offer that LSG micro supercapacitor has superior electrochemical properties rather than two previous works.

**Table 1** Comparison of the specific capacitance of LSG supercapacitors produced by various methods.

Electrode material	Specific capacitance ( $\text{F}/\text{cm}^3$ )	Reference
LSG	$\sim 2-3$	[23]
LSG	$\sim 6$	[29]
LSG	$\sim 10$	This work

## 5. CONCLUSIONS

In summary, LSG multilayer were successfully obtained by laser irradiation of LSG on the DVD disk. Raman and XPS consequences confirm that the laser irradiation properly reduce GO to graphene sheets. The performance of LSG supercapacitors as promising candidates for supercapacitor bulk electrodes and micro-supercapacitors were confirmed by galvanostatic CC and CV experiments. The present results prove that LSG flexible micro-supercapacitors offer higher specific capacity ( $8 \text{ F cm}^{-3}$ ) at both high and low current densities than pristine graphene electrodes ( $2-3 \text{ F cm}^{-3}$ ). Galvanostatic charge-discharge experiments, CV and EIS measurements were employed to characterize LSG composite as promising candidates for super capacitor bulk electrodes and micro super capacitors. The results prove that LSG flexible micro super capacitors offer higher specific capacity and better capacity retention at both high and low current densities than pristine graphene electrodes. In addition, the performance of these microsupercapacitors is still appropriate at different bending angles.

## References

- [1] D Pech, M Brunet, H Durou, P Huang, V Mochalin, Y Gogotsi, PL Taberna, Nature nanotechnology 5 (9) (2010) 651
- [2] Chmiola J, Largeot C, Taberna PL, Simon P, Gogotsi Y. Science 328 (2010) 480
- [3] Simon P, Gogotsi Y. Nat Mater 78 (2008) 45
- [4] Mai LQ, Yang F, Zhao YL, Xu X, Xu L, Luo YZ. Nat Commun 2 (2011) 381
- [5] J. M. Sieben, E. Morallón and D. Cazorla-Amorós, Energy 58( 2013) 519
- [6] J. T. Zhang, J. W. Jiang, H. L. Li and X. S. Zhao, Energy Environ Sci. 4(10) (2011) 4009
- [7] Yiqing Sun, Qiong Wu and Gaoquan Shi , Energy Environ. Sci. 4 (2011) 1113
- [8] S. Stankovich, D.A. Dikin, GH. Dommett, KM. Kohlhaas, EJ. Zimney, EA. Stach, RD. Piner, ST. Nguyen and RS. Ruoff, Nature 442 (2006) 282
- [9] JR. Miller, RA. Outlaw and BC Holloway, Science 329 (2010) 1637
- [10] A. H. Reshak and S. Auluck, RSC Adv.4 (2014) 37411
- [11] A. H. Reshak and S. Auluck, Mater. Express 4 (2014) 508

*Exp. Theo. NANOTECHNOLOGY* 3 (2019) 9-18

- [12] J. Thakur, M. K. Kashyap, H. S. Saini, A. H. Reshak, *Journal of Alloys and Compounds* 649 (2015) 1300
- [13] J. Thakur, H.S. Saini, M. Singh, A.H. Reshak, M. K. Kashyap, *Physica E* 78 (2016) 35
- [14] Aruna P. Wanninayake, Benjamin C. Church, Nidal Abu-Zahra, *Exp. Theo. NANOTECHNOLOGY* 2 (2018) 31
- [15] Y. Z. Liu, Y. F. Li, Y. G. Yang, Y. F. Wen and M. Z. Wang, *ScriptaMaterialia* 68 (2013) 301
- [16] D. R. Dreyer, S. Park, C. W. Bielawski and R. S. Ruoff, *Chem. Soc. Rev.* 39 (2010) 228
- [17] S. Alwarappan, C. Liu, A. Kumar and C. Z. Li, *J. Phys. Chem. C* 114 (2010) 12920
- [18] Mustafa M. Jaber, Ali H. al-hamdani, Yasmeen Z. Dawood, *Exp. Theo. NANOTECHNOLOGY* 2 (2018) 21
- [19] K. R. Ratinac, W. Yang, J. J. Gooding, P. Thordarson and F. Braet, *Electroanalysis* 23 (2011) 803
- [20] M.F. El-Kady, V. Strong, S. Dubin and R.B. Kaner, *Science* 335 (2012) 1326
- [21] V. Strong, S. Dubin, M.F. El-Kady, A. Lech, Y. Wang, B.H. Weiller and R.B. Kaner, *ACS Nano* 6 (2012) 1395
- [22] M.F. El-Kady and R.B. Kaner, *ACS Nano* 8 (2014) 8725
- [23] M.F. El-Kady and R.B. Kaner, *Nat. Comm.* 4 (2013) 1475
- [24] H. Tian, Y. Yang, D. Xie, Y.L. Cui, W.T. Mi, Y. Zhang and T.L. Ren, *Sci. Rep.* 4 (2014) 3598
- [24] H. Tian, C. Li, M. A. Mohammad, Y. L. Cui, W. T. Mi, Y. Yang, D. Xie and T. L. Ren, *ACS Nano*, 8 (6) (2014) 5883
- [26] H. Tian, Y. Shu, X.F. Wang, M.A. Mohammad, Z. Bie, Q.YiXie, C. Li, W.T. Mi, Yi Yang and T.L. Ren, *Sci. Rep.* 5 (2015) 8603
- [27] H Tian, Y. Shu. Y.L. Cui, W.T. Mi, Y. Yang, D. Xie and T.L. Ren, *Nanoscale* 6(2)(2014) 699
- [28] K. Griffiths, C. Dale, J. Hedley, M.D. Kowal, R.B. Kaner and N. Keegan, *Nanoscale* 6 (2014) 13613
- [29] Z. Li, P. Liu, G. Yun, K. Shi, X. Lv, K. Li, J. Xing and B. Yang, *Energy* 69 (2014) 266
- [30] Y. L. Chen, Y. Q. Chang, H. W. Wang, Z. Y. Zhang, Y. Y. Yang and H. Y. Wu, *The J. Phys. Chem. C* 115 (2011) 2563